ELSEVIER

International Journal of Pharmaceutics 131 (1996) 103–115

international journal of pharmaceutics

Research Papers

A lamellar matrix model for stratum corneum intercellular lipids. I. Characterisation and comparison with stratum corneum intercellular structure[1]

Hamid R. Moghimi, Adrian C. Williams, Brian W. Barry*

Postgraduate Studies in Pharmaceutical Technology, The School of Pharmacy, University of Bradford, Bradford, BD7 1DP, UK

Received 26 May 1995; accepted 12 July 1995

Abstract

The principal barrier to transdermal delivery of most drugs is the lamellar intercellular lipid matrix of the stratum corneum (SC). Preparation of a model for this matrix provides opportunities to probe the nature of the SC barrier. Here, a method has been developed to construct a model matrix comprising 20% cholesterol, 25% water and 55% SC free fatty acids and their soaps. X-ray diffraction studies revealed that the model matrix consists of both lamellar gel (L_β) and lamellar liquid crystalline (L_α) phases and possibly some crystalline lipids at ambient temperature, in good agreement with SC intercellular lipids structure. The matrix provided a lamellar mesomorphic structure from ambient to almost 100°C, a hexagonal mesomorphic phase at around 105°C and an isotropic liquid at 140°C as studied by hot-stage polarised light microscopy (PLM). The matrix showed seven endothermic transitions in differential scanning calorimetry (DSC) from −30 to 120°C which were well correlated with PLM results and human SC data. DSC results also revealed that around 20% of the total water in the matrix was bound. These studies have provided a simple matrix which models the lipid domain of human SC and should be useful in probing the barrier nature of SC and drug and enhancer interactions with SC intercellular lipids.

Keywords: Model human stratum corneum lipid; Mesomorphic state; Lamellar structure; X-ray diffraction; Hot-stage polarised light microscopy; Differential scanning calorimetry

1. Introduction

The main barrier to transdermal delivery of most drugs is usually located at the outermost layer of the skin, the stratum corneum (Berenson and Burch, 1951). The stratum corneum (SC) is a multilayered wall-like structure in which keratin-rich corneocytes embed in an intercellular lipid-rich matrix. In this two-compartment system the only continuous phase is the intercellular domain which seems to be the major rate-determining pathway by which most drugs traverse the stratum corneum (Elias and Friend, 1975; Albery and Hadgraft, 1979; Tojo, 1987; Boddé et al., 1991).

* Corresponding author. Tel.: +44 1274 384761; Fax: +44 1274 384769.

[1] Preliminary data presented at The British Pharmaceutical Conference, Reading, UK, September 1993.

SSDI 0378-5173(95)04306-U

An organised bilayer structure for intercellular lipids was postulated by Michaels et al. (1975). Freeze-fracture electron microscopy studies of the SC (Elias and Friend, 1975; Elias et al., 1977) led to the theory that SC intercellular lipids arrange into lipid bilayers (Elias et al., 1979). In this arrangement the lipids pack into lamellae with the hydrocarbon chains mirroring each other and the polar groups dissolving in the aqueous layer.

Preparation of a model for the intercellular lipids of the SC provides opportunities to probe the barrier nature of the SC. Stratum corneum lipids mainly comprise free sterols, fatty acids, sphingolipids and triglycerides together with smaller amounts of phospholipids, sterol/wax esters, cholesteryl sulphate, squalene and *n*-alkanes (Lampe et al., 1983a). Friberg and Osborne (1985) found that neither sphingolipids nor all the lipid components of the stratum corneum form a lamellar mesomorphic structure with water. However, the condition changed when the pH of the skin (4.5–6.0), at which the fatty acids are partially neutralised, was taken into account. When 41% of free fatty acids was neutralised by NaOH, the acid/soap mixture gave a lamellar mesomorphic structure with water (Friberg and Osborne, 1985; Osborne and Friberg, 1987).

A mixture of cholesterol and ceramides was unable to form liposomes in an aqueous medium of pH 7.5, but addition of one or both of palmitic acid and cholesteryl sulphate to this system developed such structures (Wertz et al., 1986). Abraham and Downing (1989) prepared liposomes from ceramides, cholesterol, free fatty acids and cholesteryl sulphate at pH 7.0. It is clear that under these circumstances, either free fatty acids or cholesteryl sulphate, which are ionised, are responsible for bilayer formation (Wertz et al., 1986).

Friberg et al. (1988) prepared a lamellar mesomorphic structure from fatty acids/soaps:cholesterol (19:14, w/w) and water (32%, w/w). Addition of ceramides and oleic acid palmityl ester changed the system to a two-phase mixture of which one was mesomorphic. Further addition of squalene gave a mesomorphic phase with a liquid dispersed in it.

It has been argued that as far as the barrier property of intercellular lipids is concerned, the presence of a mesomorphic structure plays the major role in barrier performance and the differences in barrier property with specific lipid change may be negligible (Friberg and Kayali, 1989; Kayali et al., 1991). Based on the above references, a simple model matrix containing 20% cholesterol, 25% water and 55% (w/w) free fatty acids and their soaps was prepared here. The matrix was then characterised by X-ray diffraction, hot-stage polarised light microscopy and differential scanning calorimetry studies.

2. Materials and methods

2.1. Materials

All materials were used as received. Table 1 provides the sources and purities of fatty acids, cholesterol and antioxidants used in this work. All other solvents and reagents were of analytical grade.

2.2. Preparation of the model matrix

Table 1 shows the composition of the model matrix prepared in this study. Fatty acids were in the same composition as they occur in abdominal SC (Lampe et al., 1983b). To prepare a lamellar structure, 41% of fatty acids was neutralised by NaOH as done by Friberg and Osborne (1985), but instead of centrifugation through a constricted glass tube (see Friberg and Osborne, 1985), a hand-shaking method, normally used to prepare liposomes (New, 1990), was employed here with slight modification. This method involves solvent evaporation and lipid hydration. Performing these processes above the transition temperature of lipids increases the evaporation efficiency and facilitates hydration. The main transition temperature of the lipid mixture containing fatty acids and cholesterol was measured by differential scanning calorimetry (as explained later) to be around 40°C and, accordingly, the matrix was prepared as follows.

Table 1
Composition of the model matrix prepared

Component	Source	Purity (%)	wt% in the matrix	
Fatty acids[a]			55	
Stearic acid	Aldrich[b]	99+		5.4
Palmitic acid	Sigma[c]	99		20.3
Myristic acid	Sigma	99+		2.1
Oleic acid	Sigma	99		18.3
Linoleic acid	Sigma	99		6.9
Palmitoleic acid	Sigma	99		2.0
Cholesterol	Aldrich	99+	20	
Butylated hydroxyanisole	Sigma	98	0.01	
Butylated hydroxytoluene	Sigma	98	0.01	
Water			25	

[a]41% of fatty acids were neutralised by NaOH to prepare their soaps.
[b] Aldrich Chemical Company (Dorset, England).
[c]Sigma Chemical Company (Dorset, England).

From a solution of lipids in a mixture of chloroform-methanol (2:1 v/v) in a 250-ml round bottom flask, the solvent was evaporated using a rotatory evaporator, initially at 30°C until a lipid film deposited on the walls of the flask and continued for another 15 min, and then at 42–43°C for 45 min under a vacuum of 450–700 mmHg. An aqueous solution of NaOH together with glass beads was added to the lipid mixture and the flask was sealed. The fatty acids were then neutralised and the lipids hydrated by mixing materials, initially at 45°C by rotator and then by hand-shaking at room temperature. Antioxidants were added as solutions in methanol during the preparation of the lipid mixture to give final concentrations of 0.02% (w/w) in the matrix. All glassware was rinsed with ether prior to use to prevent external lipid contamination.

2.3. Thermogravimetric analysis

To evaluate the efficiency of solvent evaporation from the lipid mixture and also the water content of the model matrix, thermogravimetric analysis (TGA) on samples of 10–30 mg lipid mixture and matrix were performed using a 7 Series Thermal Analysis System (Perkin Elmer, USA) over different temperature ranges from room temperature to 250°C at a heating rate of 5°C min^{-1}.

2.4. Karl Fischer titration

Karl Fischer titration (KFT) experiments were performed on a 701 KF Titrino (Metrohm Ltd., Switzerland) to determine the water content of the model matrix. Due to slow dissolution of matrix in the KF reagent, different methods were investigated and the following procedure was found to be suitable. Matrix samples were titrated continuously for 30 min to ensure complete dissolution of the matrix in the KF medium and the results were corrected for the effect of atmospheric humidity during this long procedure using a blank.

2.5. X-ray diffraction

The X-ray diffraction technique is useful for structure analysis of mesomorphic systems (e.g., see Luzzati, 1968; Small, 1986). Here, X-ray diffraction experiments were performed using a Stoe Stadi-P diffractometer (Germany). These experiments used a KαCu radiation with a wavelength of 1.541 Å.

Samples of the model matrix were sandwiched between two sheets of plastic film in a standard transmission sample holder and data were collected at ambient temperature in the 2θ range of 1–30° (where θ is the scattering angle) with a step size of 0.1° 2θ and a count time of 10 s per step. Samples were rotated continuously in the X-ray beam for the duration of the experiment.

2.6. Hot-stage polarised light microscopy

The mesomorphic structure of the matrix was assessed in cross-polarised light using a Labophot-2A light microscope (Nikon, Japan) connected via a 109 digital display (Colorado Video Inc., USA) to a video cassette recorder (Mitsubishi, Japan), a JVC monitor and a colour video copy processor (Mitsubishi, Japan). The thermal behaviour of matrices between −30 and 160°C was studied using a Stanton Redcroft heating-freezing stage (England) with a heating rate of 5°C min^{-1}.

2.7. Differential scanning calorimetry

Differential scanning calorimetry (DSC) was performed using a 7 Series Thermal Analysis System (Perkin Elmer, USA). Samples of 5–15-mg matrices were placed in hermetically-sealed large volume stainless steel capsules and their thermal behaviour studied over the ranges of −30–120 and 10–120°C at a heating rate of 5°C min^{-1}. The capsules suppress the vaporisation of volatile materials and thereby eliminate the interfering effects of the heat of vaporisation. The thermal behaviours of the lipid mixture and cholesterol were studied over the temperature ranges of 10–150 and 25–170°C, respectively, at a heating rate of 5°C min^{-1}. The enthalpy of fusion of ice was also measured by DSC using deionised double distilled water.

3. Results and discussion

3.1. Thermogravimetric analysis and Karl Fischer titration

Thermogravimetric analysis on the lipid mixture before hydration showed a negligible rate of weight loss per minute up to 150°C and a total weight loss of only 0.5% from 25 to 150°C, indicating efficient evaporation of the solvents in the preparative procedure. TGA and KFT revealed a water content (mean ± S.D.) of 24.7 ± 1.3%, n = 9 and 24.5 ± 1.6%, n = 10, respectively, which values are in good agreement with the theoretical expected amount of water in the system (25%, w/w) indicating negligible water loss during matrix preparation.

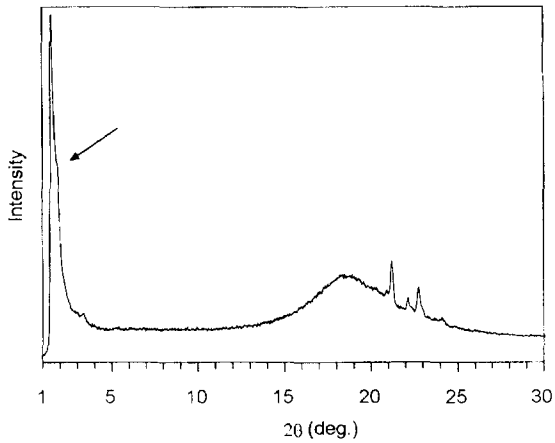

Fig. 1. X-ray diffraction profile of the model matrix at ambient temperature. The shoulder at 2θ = 2.34° is illustrated by an arrow.

3.2. X-ray diffraction

Fig. 1 shows a sample profile of reflection intensity versus 2θ and Table 2 summarises the X-ray reflections of the matrix at ambient temperature. The scattering angle (θ) is related to the repeat

Table 2
Summary of X-ray diffraction patterns of the matrix at ambient temperature

2θ (deg.)	Repeat distance (Å)	Relative intensity (%)
1.70	52.0	100
2.34	37.8	11
3.38	26.1	3.5
18.2	4.87	19
18.7	4.74	18
19.2	4.62	17
19.8	4.49	14
20.2	4.39	14
21.1	4.20	22
21.6	4.11	6.9
22.0	4.03	9.5
22.7	3.92	13
23.2	3.83	3.8
23.6	3.76	3.6
24.0	3.70	3.9

distance (d) by the Bragg equation. Here, the position of the reflections will be denoted by both the repeat distance and 2θ.

The model matrix showed a sharp interference in the small angle region (2θ = 1.70°, d = 52.0 Å). This band was accompanied by a shoulder at 2θ = 2.34° (d = 37.8 Å). The matrix also showed an interference at 2θ = 3.38° (d = 26.1 Å) in the small angle area. In the high angle region, the matrix provided a diffuse band around 2θ = 19° with d-spacing of around 4.6 Å. Three other sharp bands were seen in the high angle region at 2θ of 21.1, 22.0 and 22.7° corresponding to d-spacings of 4.20, 4.03 and 3.92 Å respectively. Some other bands were also revealed in the high angle region which are also listed in Table 2.

Analysis of small angle reflections (2θ < 10°) allows us to determine the symmetry and dimension of the lattice and the reflections or diffuse bands in the high angle region provide information concerning the conformation of hydrocarbon chains (Luzzati and Tardieu, 1974).

The sharp interference at a small angle determines the dimension of the lattice (d = 52.0 Å), assuming that the main position of this peak is first order, and the diffuse band at around 2θ = 19° ($d \cong$ 4.6 Å) shows that the hydrocarbon chains are highly disordered (type α). The reflections at 52.0 and 26.1 Å in the model matrix yield the ratio of 1:1/2 that is characteristic of a lamellar periodicity (Fig. 2a) (Luzzati, 1968; Luzzati and Tardieu, 1974). A unit cell with repeat distance of 52.0 Å (based on the assumption that the position of the sharp peak at 2θ = 1.70° is of first order) and even 104 Å (assuming that the position of the sharp peak at 2θ = 1.70° is of second order) cannot be used to explain the

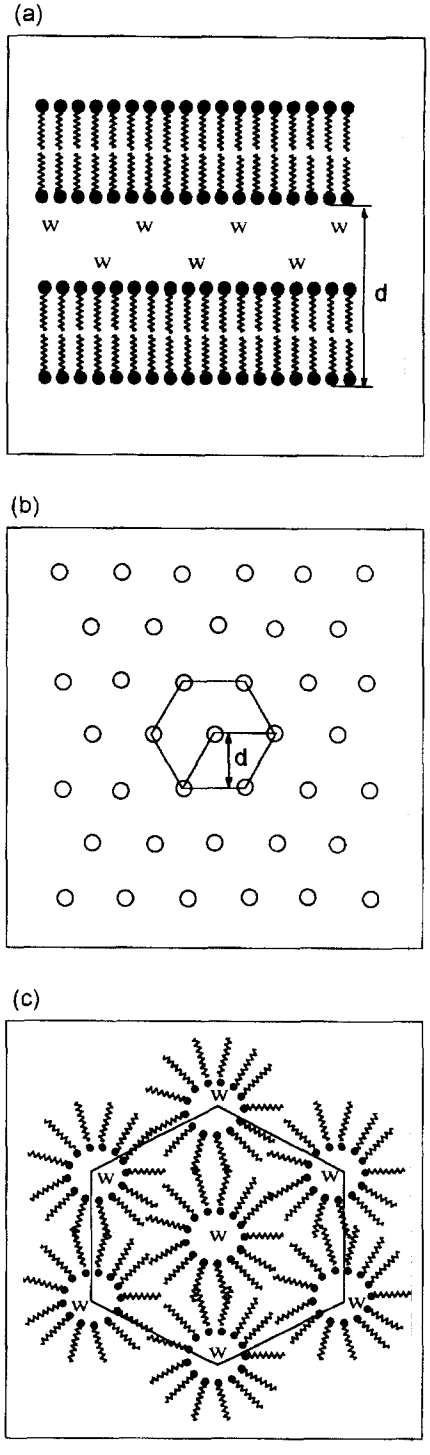

Fig. 2. Schematic representation of lamellar (neat) and hexagonal (middle) mesomorphic structures. (a) Section perpendicular to the lamella in the neat phase. (b) Section parallel to the lamella, in the middle of the lipid layer, showing the hexagonal packing of the hydrocarbon chains in a lamellar gel (L_{β}) phase. (c) Section perpendicular to the rod axis in a reversed hexagonal phase. The hydrophilic groups and hydrocarbon chains are represented by solid circles and zigzag lines, respectively. The regions containing the aqueous solvent are denoted by the w's. 'd' represents the repeat spacings (see text) (after Vincent and Skoulios, 1966; Luzzati, 1968).

source of the shoulder at $2\theta = 2.34°$ ($d = 37.8$ Å). Therefore, this shoulder should be based on another repeating unit and it is possible that this peak is a second order diffraction peak of a unit cell with $d = 75.6$ Å.

The presence of sharp bands in the high angle region indicates that some of the hydrocarbon chains of the model matrix are stiff and fully extended. The reflections of 4.20 and 4.11 Å may indicate that hexagonal (Fig. 2b) and/or pseudo-hexagonal nonspecific alkyl chain packings (type β) are present in the model matrix (Luzzati and Husson, 1962; Luzzati, 1968; Luzzati and Tardieu, 1974; Small, 1986). The band at 3.92 Å may arise from a specific tight alkyl chain packing (crystalline lipids) probably with triclinic or orthorhombic perpendicular arrangement (Small, 1986; Cornwell et al., 1994).

The present X-ray results indicate that the structure of the lipids in the model matrix possibly consists of domains built up of two unit cells with repeat distances of 52.0 and 75.6 Å and both lamellar gel (L_β) and lamellar liquid crystalline (L_α) phases and possibly some crystalline lipids are present in this system at ambient temperature.

Small angle X-ray studies of hydrated human SC (Bouwstra et al., 1991a; Bouwstra et al., 1991b) showed a profile similar to that of our model matrix in the small angle region and that SC lipids are arranged in two lamellar structures (in correlation with our data) with repeat distances of 65 and 134 Å at ambient temperature. The lamellar periodicity of 52.0 Å (and a possible periodicity of 75.6 Å) in our model matrix are different from those of SC intercellular lipids reported by Bouwstra and co-workers, which is not surprising as our model is simple and does not contain some SC lipids including ceramides of very long chain length (C_{24}–C_{35}). Absence of the SC repeat distance of 134 Å in a model matrix comprising fatty acids/soaps, cholesterol and ceramides has also been reported by Schückler et al. (1993).

Wide angle X-ray diffraction studies of human SC at ambient temperature showed different sharp intense reflections at 5.75–5.72, 5.14, 5.03, 4.89–4.86, 4.16–4.12 and 3.74–3.71 Å and medium or weak intensity diffraction lines at 3.04–3.03 Å related to lipids (Bouwstra et al., 1992; Cornwell et al., 1994). According to these bands, it has been suggested that alkyl chains of the SC lipids are arranged in orthorhombic perpendicular and (pseudo) hexagonal (gel phase) packings. It has also been argued that cholesterol is probably also present in the form of small crystals in human SC (Bouwstra et al., 1992; Cornwell et al., 1994). Some of these bands are seen in our model matrix (Table 2) and, as explained earlier, our matrix shows the nonspecific hexagonal or pseudo hexagonal and possibly the specific triclinic or orthorhombic perpendicular arrangements of alkyl chains, in good agreement with the human SC data. The broad diffuse band of around 4.6 Å in the model matrix (Fig. 1) is also reported for human SC and is attributed to both hydrocarbon chains in the liquid state (type α) and soft keratin located in the corneocytes (Bouwstra et al., 1992). Note that there is no keratin in our model system.

Small angle X-ray diffraction studies of murine SC at 25°C showed a lamellar structure with a repeat period of 131 Å (White et al., 1988) which is absent in our matrix. In the wide angle region, the murine SC revealed two sharp bands at 3.75 and 4.16 Å and a diffuse band at about 4.6 Å (all present in our model matrix, Table 2). This observation was interpreted to mean that crystalline and liquid alkyl chains coexist in the structure (White et al., 1988) which correlates with the above mentioned human SC and our model matrix results.

A lamellar structure obtained from fatty acids:cholesterol: phosphatidylethanolamine (19:14:5, w/w) and water was prepared by Friberg et al. (1988) after partial neutralisation of fatty acids. The interlayer spacing of this mesomorphic structure was studied as a function of water content from 30 to 40% (w/w) water by small angle X-ray experiments (Friberg et al., 1988). Extrapolation of Friberg and co-workers' results to a water content of 25% (the water content of the present model matrix) gave an interlayer spacing of 53.6 Å which is in reasonable correlation with our matrix results at small angle area ($d = 52.0$ Å).

3.3. Hot-stage polarised light microscopy

The model matrix showed different textures of neat phase (oily streaks, positive units and mosaic

texture which itself is a network of positive and negative units) representative of lamellar structure, from ambient temperature to almost 100°C. Here the term 'texture' is used for microscopic appearance and 'structure' for molecular arrangements of lipids, as employed by Rosevear (1954). At 25 and 32°C (SC temperature) the matrix showed an oily streaks texture in a planar matrix (Fig. 3a). This texture was normally accompanied by a mosaic texture (Fig. 3b). Apparently the mechanical disturbance of matrices by glass coverslips during sample preparation is partly responsible for some planar patches changing to the mosaic texture.

During the heating process, the first signs of a textural change appeared at around 35°C, where positive units started to grow in planar areas (compare Fig. 3a, c and d). The planar areas appear to be isotropic under cross polars, but they represent not truly isotropic liquid as they change to a mosaic texture on heating. Besides the major textural change (mosaic growth), a minor change was also observed around 35°C as some fine mosaic grains disappeared from the system.

Between 40 and 50°C, more mosaic textures grew (quite rapidly) in the system (compare Fig. 3e and b) and these textures became dominant. During heating to higher temperatures, the mosaic texture continued to extend in the system and gradually replaced the oily streaks and planar areas until around 95°C where all planar areas and oily streaks changed to mosaic texture (compare Fig. 3f and g with a).

With further heating, the matrix showed fanlike and angular textures (Fig. 3h) at around 105°C which are representative of hexagonal mesomorphic structures. The hydrocarbon chain mobility increases upon heating and a reversed hexagonal phase (H_{II}, Fig. 2c) is favourable for such thermal movement (Larsson and Lundström, 1976). These textures faded with further temperature increase and the system formed an isotropic liquid at around 140°C.

When the model matrix was frozen for subambient polarised light microscopy studies, the matrix brightness decreased and some dark green-yellow colours appeared in the system. During heating from −30°C to higher temperatures, the first textural change was a sudden increase in the brightness of the model matrix and disappearance of the colours at 0°C (pictures not shown). To find the reason for this textural change, the melting of ice under cross-polarised light in our apparatus was studied. Results showed that when water changes to ice, the ice crystals show a coloured pattern very similar to that of the frozen matrix and this pattern disappears after melting of ice. No further changes in the texture of the model matrix was seen on further heating of the matrix from 1 to 25°C. The textural changes of the frozen matrix from 25°C until the end of experiment (160°C) were similar to those of the unfrozen samples as explained above.

3.4. Differential scanning calorimetry

DSC studies of the model matrix were performed over two different temperature ranges. Here, in explanation of DSC results, the term 'frozen' will be applied to the samples that were studied from −30 to 120°C and the expression 'unfrozen' used for those observed over the range 10–120°C.

The matrix showed seven endothermic transitions (T_1–T_7) from −30 to 120°C (Fig. 4 and Table 3). Addition of 0.02% (w/w) antioxidants did not change the DSC thermal profile of the matrix.

The first endothermic transition of the matrix (T_1, −11.5°C) may represent melting of some fatty acids chains (linoleic acid melts at −12°C). As explained earlier, no textural change was seen around the T_1 transition in polarised light microscopy.

Transition T_2 (−1.7°C) obviously arises from the ice melting as shown by polarised light microscopy. The enthalpy of fusion of ice was measured here by DSC using deionised double distilled water to be 321.9 ± 1.8 J g^{-1} (these and all such subsequent data represent mean ± SD, $n = 3$). We assumed that the free water in the matrix behaves like pure water and using the enthalpy of melting of ice and that derived from T_2 (64.7 J g^{-1}), calculated that around 20% of the total water in the matrix was bound. This implies that intercellular lipids can also participate in the bound water-holding capacity of the stratum

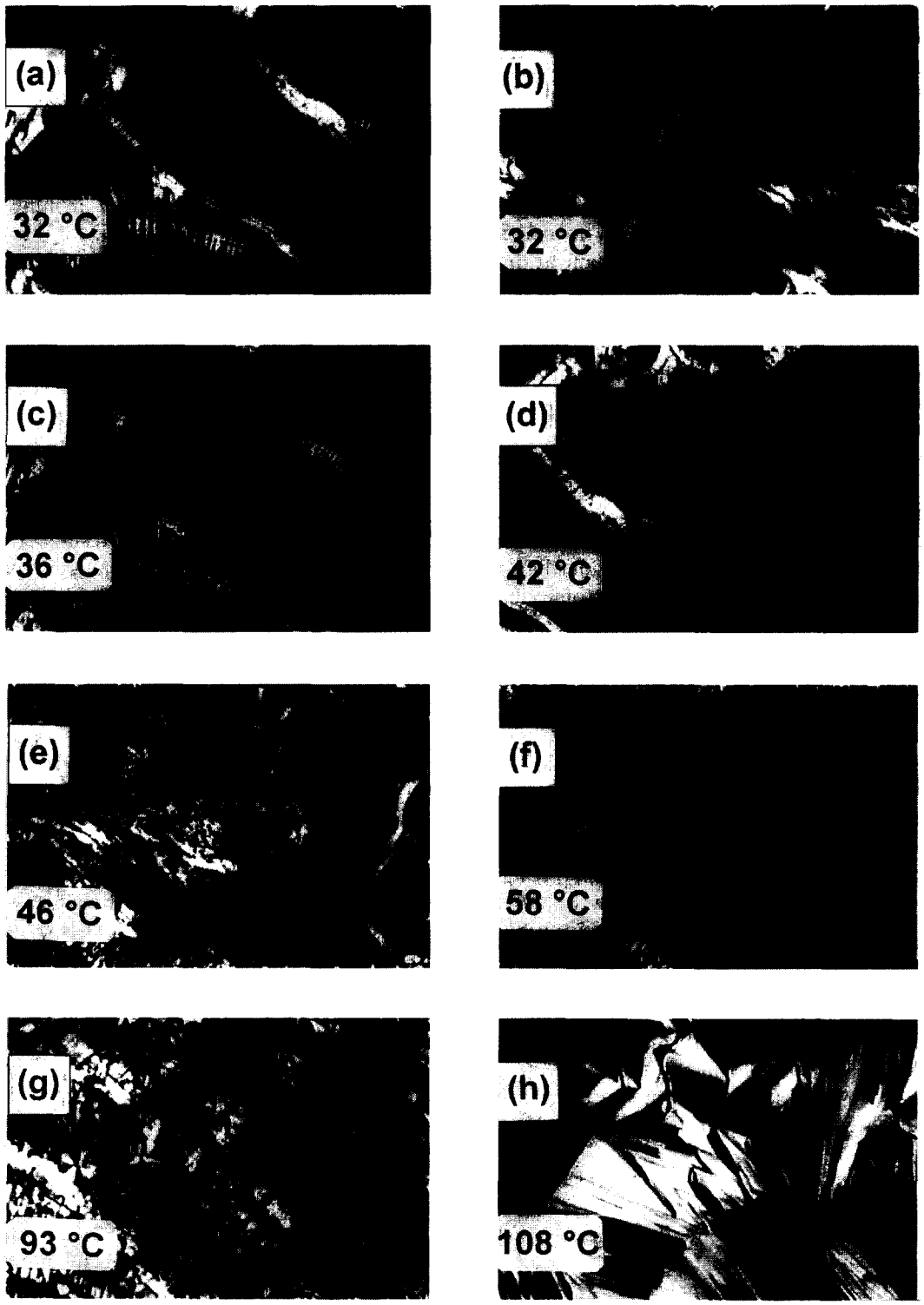

Fig. 3. Photographs illustrating the textures of the model matrix in cross polarised light. Oily streaks in planar area (a) and mosaic texture (b) indicating the lamellar structure of the model matrix at 32°C. Positive units start to grow at around 35°C; (c) a sample at 36°C; (d) a sample at 42°C. More mosaic texture and positive units grow in the system during heating to higher temperatures; (e) a sample of mosaic texture at 46°C; (f) a sample of mosaic texture and oily streaks in planar matrix at 58°C. All planar areas and oily streaks change to mosaic texture at around 95°C; (g) a sample at 93°C. The matrix changes from lamellar to hexagonal at around 105°C; (h) a sample at 108°C showing fanlike and angular textures of hexagonal liquid crystalline structure.

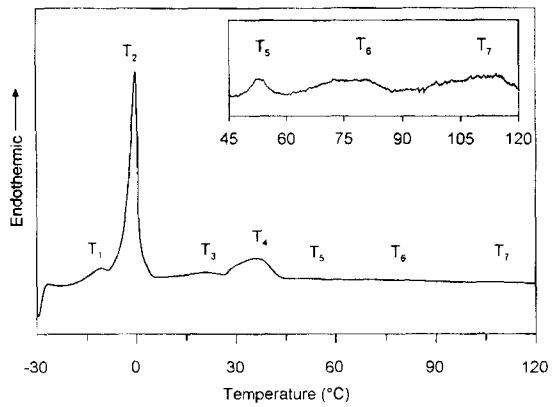

Fig. 4. Differential scanning calorimetry profile of the model matrix showing seven endothermic transitions from −30 to 120°C. Area covering T_5, T_6 and T_7 is rescaled (small box) and shows lower enthalpies of these peaks in comparison to main peaks.

corneum, a phenomenon which is reported for human SC intercellular lipids (Imokawa et al., 1991).

The fourth endothermic thermal transition (T_4) was seen within the range of approximately 25–45°C. The mid-point (peak) of T_4 transition was 35.1°C in frozen and 35.8°C in unfrozen samples. The enthalpies of T_4 in frozen and unfrozen samples were 17.1 and 15.8 J g^{-1}, respectively.

The transition T_4 is possibly due to two structural changes in the model matrix. Firstly, as illustrated by hot-stage microscopy, positive units start to appear at approximately 35°C (peak of T_4 in DSC) and at the end of T_4 (45°C) considerable mosaic texture has appeared in the system. The mosaic texture represents the maximum degree of possible disorder in the neat phase which is the opposite extreme of the planar arrangement (Rosevear, 1954). DSC experiments on the lipid mixture before hydration showed an endothermic transition at 40.8 ± 0.6°C. These transitions may correlate with the melting of hydrocarbon chains and therefore T_4 might arise in part from gel (L_β) to liquid crystalline (L_α) phase transition. On the other hand, polarised light microscopy studies showed that besides the mosaic texture growth, some grains of fine, mosaic texture also disappeared around 35°C. As it is difficult to distinguish the grains of fine mosaic texture from those of crystalline material, this textural change is possibly due to one or both of solid-to-liquid and lamellar mesomorphic-to-isotropic phase transitions.

Anhydrous cholesterol shows an endothermic transition around 35°C which is a polymorphic crystalline transition (Loomis et al., 1979). To estimate if the T_4 transition of the model matrix arises in part from a cholesterol transition, the thermal behaviour of anhydrous cholesterol from 25 to 170°C was also studied by DSC. Cholesterol showed two endothermic transitions at 35.9 ± 1.1 and 148 ± 0°C with transition enthalpies of 6.94 ± 0.41 and 65.8 ± 0.2 J g^{-1}, respectively. Our model matrix has 20% (w/w) cholesterol. Even if we consider that all of the cholesterol in our

Table 3
Transition temperature and enthalpies of endothermic transitions of the matrix observed in differential scanning calorimetry over temperature ranges of −30–120 and 10–120°C

Transition	Transition temperature (°C)			Transition enthalpy (J g^{-1})		
	−30–120	10–120	*P* value	−30–120	10–120	*P* value
T_1	−11.5 ± 1.1 (12)	—	—	7.59 ± 0.78 (12)	—	—
T_2	−1.7 ± 0.4 (12)	—	—	64.7 ± 3.6 (12)	—	—
T_3	21.6 ± 1.0 (12)	21.8 ± 0.4 (18)	0.53	5.40 ± 0.89 (12)	1.33 ± 0.45 (18)	0.00
T_4	35.1 ± 0.4 (12)	35.8 ± 1.2 (18)	0.06	17.1 ± 1.4 (12)	15.8 ± 1.5 (18)	0.02
T_5^a	52.8 ± 3.1 (9)	55.6 ± 2.9 (18)	0.03	0.42 ± 0.25 (9)	0.46 ± 0.31 (18)	0.74
T_6^a	79.3 ± 1.5 (10)	77.8 ± 3.1 (15)	0.17	1.69 ± 1.01 (10)	1.95 ± 1.96 (15)	0.70
T_7^a	108 ± 3 (7)	105 ± 3 (8)	0.13	1.64 ± 0.82 (7)	2.50 ± 1.11 (8)	0.11

Data are summarised as mean ± S.D. (n). *P* values represent the smallest value for the level of significance for which the null hypothesis can be rejected in two-tailed t-test analysis. Null hypothesis: values of two scanning ranges are the same.
[a]Were not explicit in some samples.

matrix is in the crystalline state, the enthalpy of T_4 arising from this cholesterol change could not be more than 1.39 J g^{-1} while the enthalpy of T_4 in the matrix (in unfrozen samples) is approximately 16 J g^{-1}. This shows that the T_4 transition is not essentially a polymorphic crystalline transition of cholesterol.

A minor transition (T_3) was seen at 21.6°C in frozen and 21.8°C in unfrozen samples. This transition showed enthalpies of 5.40 and 1.33 J g^{-1} in frozen and unfrozen samples, respectively. There was no textural changes in the model matrix in polarised light around the T_3 transition, therefore it is difficult to judge the nature of this transition. The T_3 transition can be assumed to be a pre-transition endotherm for the main T_4 transition, i.e., a structural transformation in the gel (L_β) phase. However, as shown by X-ray studies, our matrix exists as a mixture of gel and liquid crystalline phases at ambient temperature. The lipid mixture also showed a transition temperature at 22.7 ± 0.3°C. Therefore, it is possible that T_3 arises from a gel (L_β) to a liquid crystal (L_α) transition.

There are another three transition temperatures (T_5, T_6 and T_7) which because of their low enthalpies can easily be missed and confused with slight baseline instability (Fig. 4 and Table 3). These transitions did not appear in some of the matrix samples studied. However, their transition temperatures were reproducible (when they appeared) and correlated well with microscopic observations.

T_5 extended from around 50 to 60°C and showed a transition temperature of 52.8°C with an enthalpy of 0.42 J g^{-1} in frozen samples. The transition temperature and enthalpy of T_5 in unfrozen samples were 55.6°C and 0.46 J g^{-1}, respectively.

The sixth endothermic transition in the model matrix (T_6) extended from about 60 to around 90°C with transition temperature and enthalpy of 79.3°C and 1.69 J g^{-1}, respectively, in frozen matrices. The unfrozen matrix showed a transition temperature of 77.8°C and an enthalpy of 1.95 J g^{-1} for T_6 transition.

The lipid mixture provided a broad endothermic transition between approximately 50 and 90°C with a mid-point of 72.0 ± 0.1°C. This window covers the T_5 and T_6 transitions of the matrix. These two transitions, therefore, possibly arise from melting of alkyl chains and correlate with the growing mosaic texture (as seen in the polarised light microscopy studies) and probably represent gel-to-liquid crystalline transitions.

The last endothermic transition of the matrix (T_7), which was the most difficult to confirm, showed transition temperatures of 108 and 105°C in frozen and unfrozen samples, respectively. The enthalpy of T_7 was calculated to be 1.64 J g^{-1} in frozen and 2.50 J g^{-1} in unfrozen matrices. As was shown by hot-stage polarised light microscopy, the matrix showed fanlike and angular textures (Fig. 3h), representative of a hexagonal mesomorphic structure, at around 105°C. This feature confirms that the T_7 arises from a lamellar-to-hexagonal liquid crystalline transition.

DSC studies were performed over two temperature ranges (−30–120 and 10–120°C). Two-tailed t-test analysis (Table 3) illustrated that there was no significant difference in transition temperatures between the two temperature ranges ($P < 0.03$). However, freezing increased the enthalpy of T_3 by about 4.1 J g^{-1} ($P = 0.00$). The enthalpy of T_4 in the frozen samples is 1.3 J g^{-1} more than that of unfrozen samples. This difference is marginally significant ($P > 0.02$). The increase in the enthalpies after freezing might be due to separation of a part of water from the system.

Our DSC results correlate well with human SC transition temperatures in terms of the matrix being a model system. Goodman and Barry (1989) reported three lipid-based endothermic transitions at 38, 72 and 85°C for human SC as assessed by differential scanning calorimetry. Cornwell (1993) reported another lipid-based endothermic transition for SC at around 50°C. One of the most recent studies performed on human SC from 10 to 110°C showed four transition temperatures related to lipids at 35, 55, 65 and 80°C (Gay et al., 1994).

The first and second SC transitions (35 and 55°C) appear in our model matrix as separate transitions exactly at the same temperatures (T_4 and T_5, Fig. 4 and Table 3). However, our model does not reveal the SC transitions of around 70 and 80°C as separate peaks but provides a broad transition from 60 to 90°C with a mid-point of

approximately 79°C (Fig. 4 and Table 3). The last transition of our model, T_7, cannot be seen in the SC (even if it exists) because the SC has a transition temperature at around 100°C, with a range of approximately 90–110°C, related to proteins (Goodman and Barry, 1989) which would obscure any T_7 transition (around 105°C).

Based on X-ray diffraction studies of human SC, the transition temperature at around 35°C was attributed to a change in the alkyl chain packing of the lipids within the intercellular bilayers from an orthorhombic to a hexagonal arrangement (Bouwstra et al., 1991b; Bouwstra et al., 1992). However, from infrared spectroscopy studies, Gay et al. (1994) suggested that the 35°C transition of human SC is a solid-to-fluid phase change for a discrete subset of SC lipids and not a change in the lattice packing of the lipids. It has been suggested that this discrepancy may arise because X-ray and infrared detect different subpopulation of lipids within the SC. As explained above, the T_4 transition of the model matrix (around 35°C) is also due to more than one structural change, including the solid-to-fluid transition, in good agreement with the SC data. The second thermal transition of human SC (55°C) is suggested to be related to a loss of crystalline orthorhombic lattice structure (Gay et al., 1994). Based on X-ray diffraction studies, the third and fourth lipid-based thermal transitions of the human SC (around 70 and 80°C, respectively) are attributed to disordering of the lamellar structure and change from hexagonal packing of the lipids to a liquid phase (Bouwstra et al., 1992), i.e., from gel (L_β) to liquid crystalline (L_α) phase, in good correlation with the model matrix results.

The enthalpies of transitions in our model do not correlate with those in the SC. It was shown for stratum corneum that the enthalpy of transition at 35°C is less than the higher temperature lipid transitions and amounts to almost 7–10% of the total measured enthalpy associated with the four peaks at 35, 55, 65 and 80°C (Gay et al., 1994). In our model, however, the enthalpy of T_4 is greater than those of the higher temperature transitions and accounts for almost 90% of the total enthalpy of T_4, T_5 and T_6 (Table 3). This is not surprising, as human SC is more complex, possesses ceramides of very long chain length (C_{24}–C_{35}) which also intercalate, and there are no lipid-protein interactions in our model. However, it is possible that our model shows some of its transitions with the same source and/or nature as those in the SC at lower temperatures than the SC.

Gay et al. (1994) showed that as the SC was dehydrated below 20% (w/w), the temperature of the 35°C transition progressively increased and reached 43°C in the dry stratum corneum. This is in good agreement with the present results, as the lipid mixture (before hydration) reveals a transition at about 41°C which is higher than the T_3 transition temperature of the model matrix (about 35°C).

Finally, the presence of more than one gel-to-liquid crystalline transition in our model may indicate that the matrix is not homogeneous and consists of different ultrastructural domains; this correlates well with the heterogeneous structure of SC intercellular lipids (Gay et al., 1994).

In conclusion, a simple lamellar matrix was prepared to model the SC intercellular lipid domain using a hand-shaking method. This method was found to be easy and versatile and the thermogravimetric analysis, Karl Fischer titration and differential scanning calorimetry studies showed good reproducibility.

X-ray diffraction and polarised light microscopy studies revealed that the model matrix possesses some of structural properties of the SC intercellular lipids, including both lamellar gel and lamellar liquid crystalline phases. The thermal behaviour of the model matrix was comparable to that of human SC in terms of transition temperatures.

Our permeation and release studies using a model hydrophilic drug (5-fluorouracil) and a model lipophilic drug (oestradiol) have shown that the matrix is also a good model for the barrier properties of SC intercellular lipids. For more details regarding the barrier properties of the model matrix and the effect of geometry of the SC on percutaneous absorption of 5-fluorouracil and oestradiol, the reader is referred to our companion paper (Moghimi et al., 1996).

References

Abraham, W. and Downing, D.T., Preparation of model membranes for skin permeability studies using stratum corneum lipids. *J. Invest. Dermatol.*, 93 (1989) 809–813.

Albery, W.J. and Hadgraft, J., Percutaneous absorption: in vivo experiments. *J. Pharm. Pharmacol.*, 31 (1979) 140–147.

Berenson, G.S. and Burch, G.E., Studies of diffusion of water through dead human skin: the effect of different environmental states and of chemical alterations of the epidermis. *Am. J. Trop. Med. Hyg.*, 31 (1951) 842–853.

Boddé, H.E., van den Brink, I., Koerten, H.K. and de Haan, F.H.N., Visualization of in vitro percutaneous penetration of mercuric chloride; transport through intercellular space versus cellular uptake through desmosomes. *J. Controlled Release*, 15 (1991) 227–236.

Bouwstra, J.A., de Vries, M.A., Gooris, G.S., Bras, W., Brussee, J. and Ponec, M., Thermodynamic and structural aspects of the skin barrier. *J. Controlled Release*, 15 (1991a) 209–220. Bouwstra, J.A., Gooris, G.S., van der Spek, J.A. and Bras, W., Structural investigations of human stratum corneum by small-angle X-ray scattering. *J. Invest. Dermatol.*, 97 (1991b) 1005–1012.

Bouwstra, J.A., Gooris, G.S., de Vries, M.A., van der Spek, J.A. and Bras, W., Structure of human stratum corneum as a function of temperature and hydration: a wide-angle X-ray diffraction study. *Int. J. Pharm.*, 84 (1992) 205–216.

Cornwell, P.A., *Mechanisms of action of terpene penetration enhancers in human skin.* Ph.D. Thesis, University of Bradford, UK (1993).

Cornwell, P.A., Barry, B.W., Stoddart, C.P. and Bouwstra, J.A., Wide-angle X-ray diffraction of human stratum corneum: effects of hydration and terpene enhancer treatment. *J. Pharm. Pharmacol.*, 46 (1994) 938–950.

Elias, P.M., Brown, B.E., Fritsch, P., Goerke, J., Gray, G.M. and White, R.J., Localization and composition of lipids in neonatal mouse stratum granulosum and stratum corneum. *J. Invest. Dermatol.*, 73 (1979) 339–348.

Elias, P.M. and Friend, D.S., The permeability barrier in mammalian epidermis. *J. Cell Biol.*, 65 (1975) 180–191.

Elias, P.M., McNutt, N.S. and Friend, D.S., Membrane alterations during cornification of mammalian squamous epithelia: a freeze-fracture, tracer, and thin-section study. *Anat. Rec.*, 189 (1977) 577–593.

Friberg, S.E. and Kayali, I., Water evaporation rates from a model of stratum corneum lipids. *J. Pharm. Sci.*, 78 (1989) 639–643.

Friberg, S.E. and Osborne, D.W., Small angle X-ray diffraction patterns of stratum corneum and a model structure for its lipids. *J. Disp. Sci. Technol.*, 6 (1985) 485–495.

Friberg, S.E., Suhaimi, H., Goldsmith, L.B. and Rhein, L.L., Stratum corneum lipids in a model structure. *J. Disp. Sci. Technol.*, 9 (1988) 371–389.

Gay, C.L., Guy, R.H., Golden, G.M., Mak, V.H.W. and Francoeur, M.L., Characterization of low-temperature (i.e., $< 65°C$) lipid transitions in human stratum corneum. *J. Invest. Dermatol.*, 103 (1994) 233–239.

Goodman, M. and Barry, B.W., Action of penetration enhancers on human stratum corneum as assessed by differential scanning calorimetry. In Bronaugh, R.L. and Maibach, H.I. (Eds.), *Percutaneous Absorption, Mechanisms — Methodology — Drug Delivery*, 2nd Edn, Dekker, New York, 1989, pp. 567–593.

Imokawa, G., Kuno, H. and Kawai, M., Stratum corneum lipids serve as a bound-water modulator. *J. Invest. Dermatol.*, 96 (1991) 845–851.

Kayali, I., Suhery, T., Friberg, S.E., Simion, F.A. and Rhein, L.D., Lyotropic liquid crystals and the structural lipids of the stratum corneum. *J. Pharm. Sci.*, 80 (1991) 428–431.

Lampe, M.A., Burlingame, A.L., Whitney, J., Williams, M.L., Brown, B.E., Roitman, E. and Elias, P.M., Human stratum corneum lipids: characterization and regional variations. *J. Lipid Res.*, 24 (1983b) 120–130.

Lampe, M.A., Williams, M.L. and Elias, P.M., Human epidermal lipids: characterization and modulations during differentiation. *J. Lipid Res.*, 24 (1983a) 131–140.

Larsson, K. and Lundström, I., Liquid crystalline phases in biological model systems. In Friberg, S. (Ed.), *Lyotropic Liquid Crystals and the Structure of Biomembranes*, American Chemical Society, Washington, DC, 1976, pp. 43–70.

Loomis, C.R., Shipley, G.G. and Small, D.M., The phase behavior of hydrated cholesterol. *J. Lipid Res.*, 20 (1979) 525–535.

Luzzati, V., X-ray diffraction studies of lipid-water systems. In Chapman, D. (Ed.), *Biological Membranes; Physical Fact and Function*, Academic Press, London, 1968, pp. 71–123.

Luzzati, V. and Husson, F., The structure of the liquid-crystalline phases of lipid-water systems. *J. Cell Biol.*, 12 (1962) 207–219.

Luzzati, V. and Tardieu, A., Lipid phases: structure and structural transitions. *Ann. Rev. Phys. Chem.*, 25 (1974) 79–94.

Michaels, A.S., Chandrasekaran, S.K. and Shaw, J.E., Drug permeation through human skin: theory and in vitro experimental measurement. *AIChE J.*, 21 (1975) 985–996.

Moghimi, H.R., Williams, A.C. and Barry, B.W., A lamellar matrix model for stratum corneum intercellular lipids. II. Effect of geometry of the stratum corneum on permeation of model drugs 5-fluorouracil and oestradiol. *Int. J. Pharm.*, (1996) submitted.

New, R.R.C., Preparation of liposomes. In New, R.R.C. (Ed.), *Liposomes, a Practical Approach*, Oxford University Press, Oxford, 1990, pp. 33–39.

Osborne, D.W. and Friberg, S.E., Role of stratum corneum lipids as moisture retaining agent. *J. Disp. Sci. Technol.*, 8 (1987) 173–179.

Rosevear, F.B., The microscopy of the liquid crystalline neat and middle phases of soaps and synthetic detergents. *J. Am. Oil Chem. Soc.*, 31 (1954) 628–639.

Schückler, F., Bouwstra, J.A., Gooris, G.S. and Lee, G., An X-ray diffraction study of some model stratum corneum lipids containing Azone and dodecyl-L-pyroglutamate. *J. Controlled Release*, 23 (1993) 27–36.

Small, D.M., The physical chemistry of lipids; from alkanes to phospholipids. In Hanahan, D.J. (Ed.), *Handbook of Lipid Research*, Vol. 4, Plenum Press, New York, 1986.

Tojo, K., Random brick model for drug transport across stratum corneum. *J. Pharm. Sci.*, 76 (1987) 889–891.

Vincent, J.M. and Skoulios, A., 'Gel' et 'coagel'. I. Identification. Localisation dans un diagramme de phases et détermination de la structure du 'gel' dans le cas du stéarate de potassium. *Acta Cryst.*, 20 (1966) 432–440.

Wertz, P.W., Abraham, W., Landmann, L. and Downing, D.T., Preparation of liposomes from stratum corneum lipids. *J. Invest. Dermatol.*, 87 (1986) 582–584. White, S.H., Mirejovsky, D. and King, G.I., Structure of lamellar lipid domains and corneocyte envelopes of murine stratum corneum. An X-ray diffraction study. *Biochemistry*, 27 (1988) 3725–3732.